

MELTING OF NEPHELINE SYENITE WITH H_2O AND $\text{H}_2\text{O} + \text{CO}_2$, AND THE EFFECT OF DILUTION OF THE AQUEOUS PHASE ON THE BEGINNING OF MELTING*

G. L. MILLHOLLEN**

Department of Geochemistry and Mineralogy,
The Pennsylvania State University, University Park, Pennsylvania 16802

ABSTRACT. The addition of 50 mole percent CO_2 to the aqueous phase raises the solidus of the Blue Mountain nepheline syenite about 80° at 1 kb and 100° at 2 to 6 kb total pressure. By use of $f_{\text{H}_2\text{O}}\text{-T}$ and $\text{Pe}_{\text{H}_2\text{O}}\text{-T}$ projections of the solidus curves with nearly pure H_2O and $0.5 \text{ H}_2\text{O} + 0.5 \text{ CO}_2$, the beginning of melting is contoured at constant $f_{\text{H}_2\text{O}}$ or constant $\text{Pe}_{\text{H}_2\text{O}}$ in $\text{P}(\text{total})\text{-T}$ projection. These contours show that as the fluid phase is diluted from $X_{\text{H}_2\text{O}}$ equals 1.0 to 0.5, the solidus at constant $f_{\text{H}_2\text{O}}$ or $\text{Pe}_{\text{H}_2\text{O}}$ is raised to higher temperature and higher pressure. Contours of the solidus at constant $\text{Pe}_{\text{H}_2\text{O}}$ are used to construct $\text{T-X}_{\text{H}_2\text{O}}$ (fluid) projections at constant total pressure. These $\text{T-X}_{\text{H}_2\text{O}}$ (fluid) projections are then used to construct $\text{P}(\text{total})\text{-T}$ projections of the solidus at constant $X_{\text{H}_2\text{O}}$ (fluid) like the experimentally-determined curves but for additional values of $X_{\text{H}_2\text{O}}$. These projections show that at 5 kb total pressure, for example, the solidus is raised about 85° , if $\text{Pe}_{\text{H}_2\text{O}}$ is reduced from 5 kb to 3 kb. If $\text{Pe}_{\text{H}_2\text{O}}$ is only 1 kb at 5 kb total pressure, the solidus is about 225° higher than the solidus with nearly pure H_2O . If $X_{\text{H}_2\text{O}}$ (fluid) is reduced from 1.0 to 0.1 at 5 kb total pressure, the solidus is raised about 430° . These results indicate that the composition of aqueous fluids has a major effect on temperatures of anatexis and of magmatic crystallization.

INTRODUCTION

Most studies of melting relations of rocks have been made either under dry conditions or in the presence of excess, nearly pure water. These are limiting conditions in most natural systems. The present study examines the effect of addition of a known amount of CO_2 to the aqueous phase on the beginning of melting of nepheline syenite and represents an attempt to simulate natural conditions in which equilibrium water pressure is less than total pressure. Although the general pattern of melting relations with equilibrium water pressure less than total pressure has been outlined previously (Yoder and Tilley, 1962), this study provides an experimental determination of these relations.

Experimental procedure.—This nepheline syenite is a representative sample from the complex at Blue Mountain, Ontario, Canada (Payne, 1968; Keith, 1939) and consists of albite, microcline, nepheline, biotite, magnetite, and minor zircon. A chemical analysis and CIPW norm are given in table 1. This analysis, made largely by spectrometry, is in good agreement with a wet chemical analysis by C. O. Ingamells of a glass made from a split of this sample. The crystalline sample was ground to minus 200 mesh in a tungsten carbide Mixer Mill and was dried and stored in a dessicator.

* Contribution No. 70-6, College of Earth and Mineral Sciences, Pennsylvania State University, University Park, Pennsylvania 16802

** Present address: Department of Geophysical Sciences, University of Chicago, Chicago, Illinois 60637

TABLE 1

Chemical analysis and CIPW norm of Blue Mountain nepheline syenite starting material

Analysis*		CIPW norm	
SiO ₂	59.00	Or	27.00
Al ₂ O ₃	22.30	Ab	43.99
TiO ₂	0.02	An	2.62
Fe ₂ O ₃	1.15	Ne	21.52
FeO	0.95	Ol	0.74
MnO	0.05	Fo	(0.26)
MgO	0.20	Fa	(0.49)
CaO	0.90	Di	0.70
Na ₂ O	10.06	Wo	(0.35)
K ₂ O	4.68	En	(0.13)
Cl	0.19	Fs	(0.22)
CO ₂	0.16	Il	0.04
H ₂ O ⁺	0.37	Mt	1.67
H ₂ O ⁻	0.03	Hl	0.31
		Cc	0.36
Total	100.06	Total	99.62

* Analysis by spectrometry and flame photometry, I. A. Kilinc, analyst; except CO₂, H₂O⁺, and H₂O⁻ determined by J. B. Bodkin. Iron oxides calculated using the Fe₂O₃/FeO ratio of Nockolds' (1954) average nepheline syenite.

Experimental runs were made with 10 to 20 wt percent distilled water, with most charges containing 15 to 17 percent water. These charges were sealed in Pd₆₀-Ag₄₀ or gold capsules.

Runs with H₂O + CO₂ were made by weighing crystalline oxalic acid dihydrate, instead of water, into Pd-Ag sample capsules. Under the conditions of these runs, oxalic acid dihydrate breaks down to form a mixture containing 50 mole percent H₂O plus 50 mole percent CO₂ (Holloway, Burnham, and Millhollen, 1968). Oxalic acid dihydrate stored in a tightly closed bottle was found to be stable, but if placed in a dessicator or heated it lost H₂O (Holloway, Burnham, and Millhollen, unpub. results). Therefore, only untreated oxalic acid was used in this study. Sufficient oxalic acid was used to produce a charge consisting of about 10 wt percent H₂O, 24 percent CO₂, and 66 percent nepheline syenite. (In run D32, however, the charge contained about 3 percent H₂O and 8 percent CO₂.)

Experimental runs were made from 0.5 to 3 kb pressure in cold-seal pressure vessels (Tuttle, 1949), which were run vertically with a filler rod and with the seal below the furnace (closed end up). Runs also were made from 1 to 6 kb in internally-heated pressure vessels (Burnham, 1962; Burnham, Holloway, and Davis, 1969a), which also were run vertically. Runs were made at about 5° intervals in cold-seal vessels and 20° intervals in internally-heated vessels. Recorded temperatures are believed to be accurate to about ± 5° for cold-seal runs and about ± 10° for runs in internally-heated vessels (Millhollen, ms). Recorded pressures are believed to be accurate to ± 0.1 kb.

Beginning of melting determinations was made by identifying glass in run products with a petrographic microscope. The H_2O -bearing glass, which has a refractive index of about 1.505, has a pink tint and negative relief in an immersion oil with a refractive index near the lower indices of the minerals. Isotropism of the glass was checked with the first-order red accessory plate.

The H_2O -saturated, silicate liquidus also was determined by examining the run products with a petrographic microscope. Glasses quenched from just below the liquidus contain small, euhedral crystals of plagioclase (?), magnetite and (or) hematite, and (at 3 kb and above) biotite. Just above the liquidus, however, only small amounts of magnetite and (or) hematite remain.

Experimental results.—Run data used to delineate the melting curves are presented in table 2. Figure 1 is a P-T projection of these data points and the melting curves determined from them.

The beginning of melting with nearly pure H_2O is in good agreement with that determined to 2 kb by Barker (1965) for litchfieldite (nepheline syenite) from Litchfield, Maine. The beginning of melting obtained by Barker is at 705° at 2 kb, 760° at 1 kb, and 810° at 0.5 kb. The beginning of melting of a similar composition in the system $\text{NaAlSi}_3\text{O}_8$ – KAlSi_3O_8 – H_2O at 1 kb (750°) (Hamilton and MacKenzie, 1965) and 5 kb (635°) (Morse, 1969) is at somewhat lower temperatures than the beginning of melting determined here, probably because of the presence of anorthite molecule in the natural feldspar.

Products of runs near the solidus contain two alkali feldspars, nepheline, biotite, and magnetite, with or without glass, and minor amounts of cancrinite and zircon. Although studies of synthetic systems (Morse, 1969; Peters, Luth, and Tuttle, 1966) indicate that analcime should become stable at the solidus of nepheline syenite at some water pressure just below 5 kb, no analcime was encountered in this study to 6 kb, again probably because of the presence of anorthite molecule in the natural feldspar.

As shown in figure 1, the addition of 50 mole percent CO_2 to the aqueous phase raises the solidus appreciably. This effect is consistent with the conclusion of Wyllie and Tuttle (1959) that the solubility of CO_2 in the silicate melt is probably very low. Watkinson and Wyllie (1969) and Holloway (ms) also found that the addition of CO_2 to the aqueous phase raised the solidus of albite plus CaO and tholeiitic basalt, respectively. This behavior may change at higher pressures because Hill and Boettcher (1970) found that at pressures above 15 kb the addition of CO_2 to the aqueous phase did not raise the solidus of tholeiitic basalt significantly.

The location of the liquidus in figure 1 indicates that this composition has a melting (or crystallization) range of about 100° at pressures above 2 kb with excess, nearly pure H_2O fluid.

Application of results.—In order to illustrate further the effect of addition of CO_2 to the aqueous phase on the beginning of melting of

TABLE 2

Experimental run data

Run No.*	P (kb)	T (°C)	Time days	Fluid**	Products
B40	0.5	838	4.8	(1)	Crystals
B47	0.5	843	10.1	(1)	Crystals + glass
B37	1.0	769	7.8	(1)	Crystals
B11	1.0	773	5.7	(1)	Crystals + glass
D105	1.1	950	3.0	(1)	Crystals + glass
D121	1.0	975	2.0	(1)	Glass + oxides
B54	2.0	709	8.2	(1)	Crystals
B57	2.0	713	9.0	(1)	Crystals + glass
D285	2.0	840	4.9	(1)	Crystals + glass
D329	2.0	860	3.8	(1)	Glass + oxides
B23	3.0	688	4.9	(1)	Crystals
B36	3.0	694	9.9	(1)	Crystals + glass
D155	3.1	780	3.0	(1)	Crystals + glass
D5	2.9	800	6.1	(1)	Glass + oxides
D311	4.0	660	6.9	(1)	Crystals
D301	4.0	680	6.5	(1)	Crystals + glass
D317	4.0	760	6.9	(1)	Crystals + glass
D117	4.0	780	5.3	(1)	Glass + oxides
D277	5.3	640	9.2	(1)	Crystals (+ glass ?)
D275	5.3	660	9.2	(1)	Crystals + glass
D97	5.0	760	1.0	(1)	Crystals + glass
D129	5.0	780	5.0	(1)	Glass + oxides
D307	6.0	640	6.9	(1)	Crystals
D331	6.0	740	3.2	(1)	Crystals + glass
D279	1.0	840	9.1	(2)	Crystals
D273	1.1	860	5.0	(2)	Crystals + glass
D261	2.0	800	6.8	(2)	Crystals
D283	2.0	820	4.9	(2)	Crystals + glass
D293	3.0	780	6.7	(2)	Crystals
D291	3.0	800	6.7	(2)	Crystals + glass
D32	3.9	750	6.9	(2)	Crystals
D315	4.0	770	6.9	(2)	Crystals + glass
D257	5.5	760	6.8	(2)	Crystals + glass
D289	5.9	740	4.9	(2)	Crystals
D287	5.9	760	4.9	(2)	Crystals + glass

*Run numbers beginning with B indicate cold-seal runs; those beginning with D indicate runs in internally-heated vessels.

** (1) indicates "pure" H_2O fluid phase; (2) indicates 0.5 $H_2O + 0.5 CO_2$ fluid phase.

nepheline syenite, the following projections were constructed. Figure 2A shows the two solidus curves in f_{H_2O} -T projection. The H_2O fugacity (f_{H_2O}) at the solidus with "pure" H_2O (neglecting dissolved solids) was obtained from the tables of Burnham, Holloway, and Davis (1969b). The f_{H_2O} at the solidus with 0.5 $H_2O + 0.5 CO_2$ was obtained by multiplying f_{H_2O} for pure H_2O obtained from the above tables for the temperature and total pressure of the solidus by the mole fraction of H_2O (X_{H_2O}) in the fluid (0.5). This calculation assumes ideal mixing of H_2O and CO_2 .

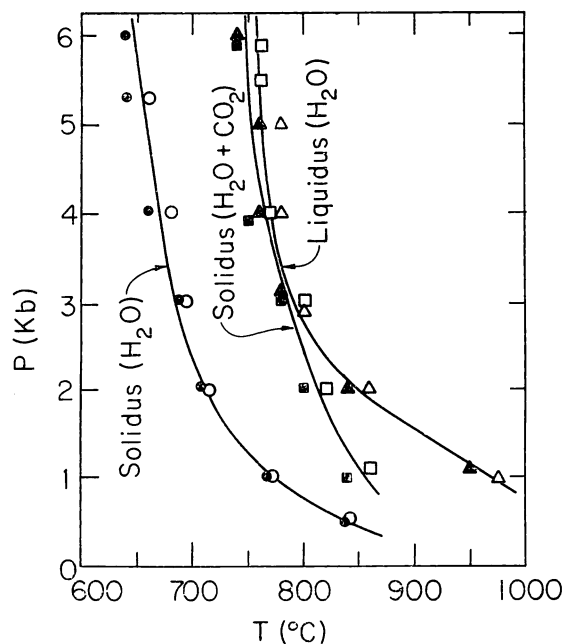


Fig. 1. P-T projection of melting relations of nepheline syenite. Filled circles indicate no glass with "pure" H_2O . Open circles and filled triangles indicate crystals plus glass with "pure" H_2O . Open triangles indicate glass plus oxides with "pure" H_2O . Filled squares indicate no glass with $0.5 \text{ H}_2\text{O} + 0.5 \text{ CO}_2$. Open squares indicate crystals plus glass with $0.5 \text{ H}_2\text{O} + 0.5 \text{ CO}_2$.

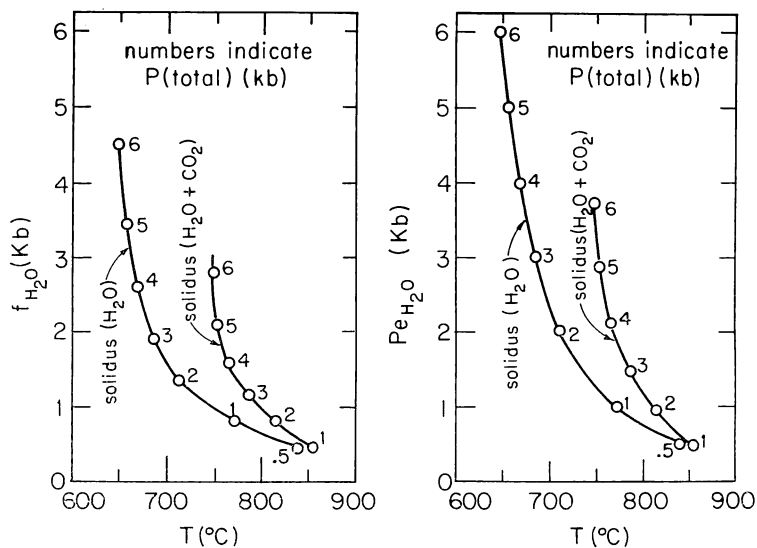


Fig. 2. Calculated solidus projections. A. $f_{\text{H}_2\text{O}}$ -T projection; B. $P_{\text{H}_2\text{O}}$ -T projection.

Figure 2B is a plot of the two solidus curves for the nepheline syenite as a function of equilibrium water pressure (P_{H_2O}) and temperature. Based on the definition by Greenwood (1961), P_{H_2O} is the pressure of pure H_2O that would be in equilibrium with H_2O in the fluid phase through a membrane permeable only to H_2O . For pure H_2O in the fluid, P_{H_2O} equals $P(\text{total})$, so the solidus with the H_2O fluid phase is the same (neglecting dissolved solids) as that given in figure 1. The P_{H_2O} at the solidus with $0.5 H_2O + 0.5 CO_2$ in the fluid was determined by the following procedure. The f_{H_2O} at a given temperature on the solidus was obtained from figure 2A. The pressure given by Burnham, Holloway, and Davis (1969b) for pure H_2O at this fugacity and temperature was the P_{H_2O} in the complex fluid.

Figures 2A and 2B may be used to contour the solidus at constant f_{H_2O} or P_{H_2O} , respectively, on a $P(\text{total})$ - T projection. The temperature at each solidus for a given f_{H_2O} (or P_{H_2O}) is obtained from figure 2A (or 2B). These two temperatures are then located on the corresponding experimentally-determined solidus curves in $P(\text{total})$ - T projection. These two points can then be connected by a curve that represents the beginning of melting at constant f_{H_2O} (or P_{H_2O}) as X_{H_2O} changes from 1.0 to 0.5 in the fluid. The resulting projections are shown in figure 3A for f_{H_2O} isobars and figure 3B for P_{H_2O} isobars. Thus, in figures 3A and 3B, the experimentally-determined solidus curves represent the beginning of

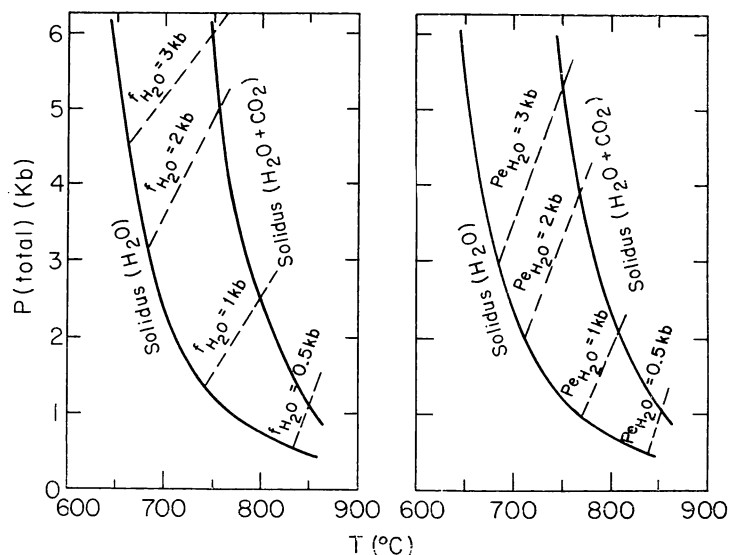


Fig. 3. $P(\text{total})$ - T projections of solidus contours. A. Solidus contours at constant f_{H_2O} together with experimentally-determined solidus curves; B. solidus contours at constant P_{H_2O} together with experimentally-determined solidus curves.

melting of the nepheline syenite at constant $X_{\text{H}_2\text{O}}$ in the fluid, whereas the contours represent the beginning of melting at constant $f_{\text{H}_2\text{O}}$ and $\text{Pe}_{\text{H}_2\text{O}}$, respectively, but with changing $X_{\text{H}_2\text{O}}$ in the fluid. These contours show that the addition of CO_2 to the aqueous phase shifts the beginning of melting at constant $f_{\text{H}_2\text{O}}$ or $\text{Pe}_{\text{H}_2\text{O}}$ to higher pressure and higher temperature. Because of the interrelationship between $f_{\text{H}_2\text{O}}$ and $\text{Pe}_{\text{H}_2\text{O}}$, either parameter could be chosen to characterize the system.

In figure 4 the solidus with nearly pure H_2O is extended to the 1 atm minimum (1020°) in the system $\text{NaAlSiO}_4\text{--KAlSiO}_4\text{--NaAlSi}_3\text{O}_8\text{--KAlSi}_3\text{O}_8$ (Schairer, 1950) and to 10 kb total pressure. A curve representing the anhydrous (dry) solidus (or the solidus with pure CO_2 , if CO_2 is insoluble in the melt) was drawn approximately parallel to the nepheline + albite melting curve (Bell and Roseboom, 1969) from the 1 atm minimum to 10 kb.

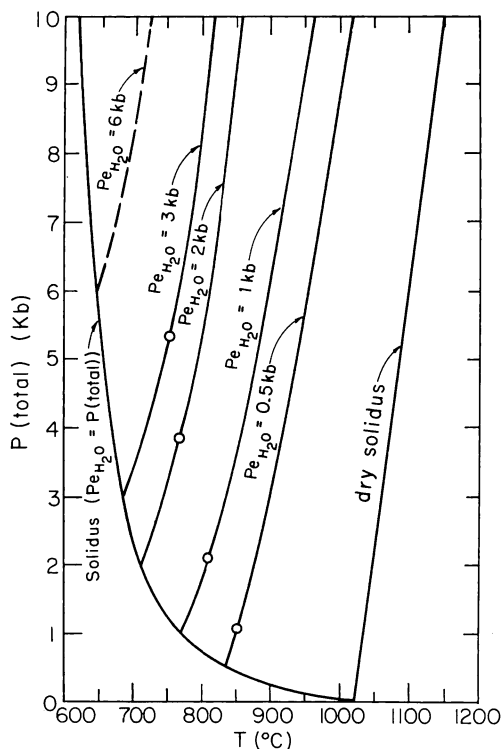


Fig. 4. $P(\text{total})\text{--}T$ projection of solidus with "pure" H_2O extrapolated to 1 atm and to 10 kb, constant $\text{Pe}_{\text{H}_2\text{O}}$ solidus contours, and dry solidus. Dry solidus was constructed parallel to nepheline + albite melting curve (Bell and Roseboom, 1969). Contour for $\text{Pe}_{\text{H}_2\text{O}} = 6$ kb was drawn from "pure" H_2O solidus at 6 kb to higher pressures after the form of the other contours. Circles represent points on experimentally-determined solidus with 0.5 H_2O + 0.5 CO_2 .

The contours in figures 3A and 3B were drawn as straight lines, arbitrarily. However, their slopes are such that they would intersect the dry solidus if extended, and therefore they must be curved. For this reason, Pe_{H_2O} contours are extrapolated in figure 4 with slopes that approach parallelism to the dry solidus. Points on the experimentally-determined solidus with $0.5 H_2O + 0.5 CO_2$ are shown as circles on the contours. For X_{H_2O} equals 1.0 in the fluid, Pe_{H_2O} equals $P(\text{total})$; therefore, the low-temperature end of each Pe_{H_2O} contour is fixed at the solidus for Pe_{H_2O} equals $P(\text{total})$.

The positions of the contours in figures 3A, 3B, and 4 are only approximations because (1) of the limits of error in location of the experimentally-determined solidus curves, (2) of the steep slopes of the projections at low temperatures in figures 2A and 2B, (3) only two points were determined experimentally for each contour, (4) the effect of solids dissolved in the fluid was neglected, and (5) of the assumption of ideal mixing of H_2O and CO_2 . However, these figures can be used for semiquantitative applications.

Figure 4 can be used to construct additional solidus curves like the experimentally-determined curves in figure 1 but for other fluid compositions. To make this construction, isobaric $T-X_{H_2O}$ (fluid) sections are first constructed. For a given total pressure, X_{H_2O} is determined at each Pe_{H_2O} contour by dividing f_{H_2O} for that Pe_{H_2O} and temperature by f_{H_2O} for pure H_2O at that total pressure and temperature, again assuming ideal mixing of H_2O and CO_2 in the fluid phase. An example of a projection obtained in this way is shown for 5 kb total pressure in figure 5. Similar projections may be made for several total pressure isobars.

For a selected value of X_{H_2O} (fluid) the temperature of the solidus for each total pressure is obtained from the $T-X_{H_2O}$ (fluid) projections and plotted on a $P(\text{total})-T$ projection. This has been done for X_{H_2O} equals 0.1 and 0.2, and the resulting curves are shown in figure 6. (Again, the location of these curves is semiquantitative because of the sources of error given above.) The two experimentally-determined solidus curves for X_{H_2O} equals 1.0 and 0.5 are also shown in this figure as is the dry (X_{H_2O} equals 0.0) solidus constructed in figure 4.

As shown in figure 6, a family of curves, each curve representing the solidus projection for a given X_{H_2O} in the fluid, extends to higher pressures from the 1 atm minimum. The slope of each of these curves depends on f_{H_2O} , which in turn is related to X_{H_2O} in the fluid. The two limiting slopes at a given pressure are represented by the dry solidus to higher temperatures and the solidus with nearly pure H_2O to lower temperatures. Thus, the slope of the solidus at constant X_{H_2O} at a given pressure in $P(\text{total})-T$ projection increases as X_{H_2O} in the fluid decreases and at some X_{H_2O} less than about 0.1 will become positive.

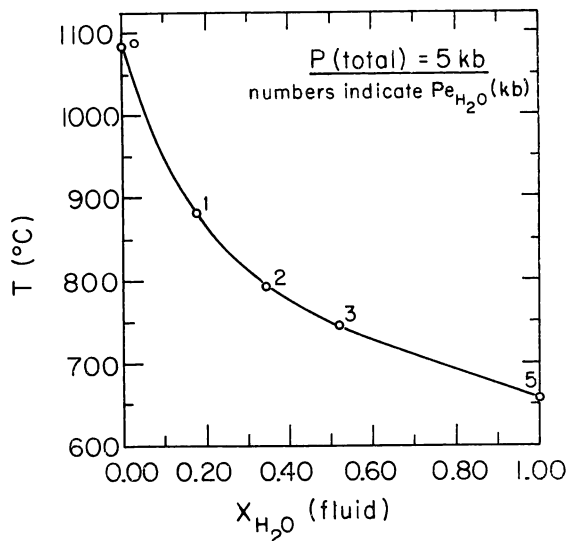


Fig. 5. Isobaric T - $X_{\text{H}_2\text{O}}$ (fluid) projection of solidus at 5 kb total pressure.

Geological applications.—Although this study was carried out with a nepheline syenite, the general role of aqueous fluid composition in magmatic processes, as illustrated here, should also be found in other silicate systems. The present results also should be applicable to systems including components other than CO_2 in the aqueous phase, if these components have a low solubility in the silicate liquid, and if they affect $f_{\text{H}_2\text{O}}$ in the same way as does CO_2 .

Figure 4 shows that at 5 kb total pressure, for example, the solidus of nepheline syenite is raised about 85° , if $P_{\text{H}_2\text{O}}$ is reduced from 5 kb to 3 kb. If $P_{\text{H}_2\text{O}}$ is only 1 kb at 5 kb total pressure, the solidus is about 225° higher than the solidus with nearly pure H_2O . Similarly, figure 6 shows that at 5 kb total pressure the solidus is raised about 100° by dilution of the aqueous phase from a mole fraction of about 1.0 to 0.5. If $X_{\text{H}_2\text{O}}$ equals 0.1 in the fluid, the solidus is about 430° higher than the solidus with nearly pure H_2O .

Therefore, the composition of pore fluids greatly influences the temperature at which anatexis begins at a given pressure. If CO_2 was present, in addition to H_2O , during formation of a migmatite, a greater temperature of formation at a given depth is indicated as compared with the temperature inferred by assuming a pure H_2O fluid. However, the shape of the solidus in T - $X_{\text{H}_2\text{O}}$ (fluid) projection (fig. 5) indicates that a small amount of CO_2 added to the aqueous phase has a lesser effect on the beginning of melting than does the same amount of H_2O added to a pure CO_2 phase; a small amount of H_2O lowers the melting temperature more than an equal amount of CO_2 raises it.

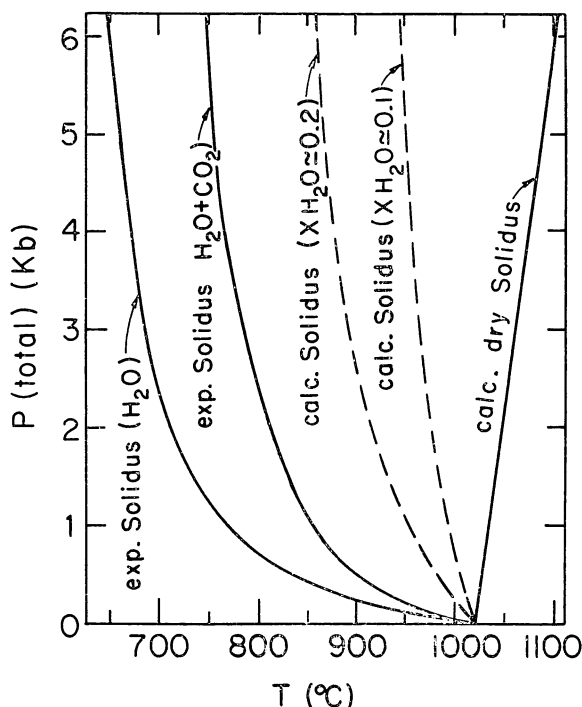


Fig. 6. $P(\text{total})$ - T projection of experimentally-determined solidus curves for $X_{H_2O} = 1.0$ and $X_{H_2O} = 0.5$, calculated solidus curves for $X_{H_2O} = 0.2$ and $X_{H_2O} = 0.1$ (see text), and calculated dry ($X_{H_2O} = 0.0$) solidus. Dry solidus was drawn parallel to nepheline + albite melting curve (Bell and Roseboom, 1969).

As melting proceeds in the presence of an $H_2O + CO_2$ fluid, H_2O is preferentially dissolved in the liquid, and the fluid is enriched in CO_2 , thereby further reducing $P_{e_{H_2O}}$ (Burnham, 1967). The amount of fluid relative to silicates will influence the amount by which $P_{e_{H_2O}}$ is lowered. The degree of lowering of $P_{e_{H_2O}}$, in turn, controls the amount by which the liquidus is raised.

These results indicate that if a H_2O -bearing magma encounters carbonate or a CO_2 -rich pore fluid, H_2O will tend to diffuse out of the magma to reach equilibrium with the fluid (Wyllie and Tuttle, 1960), and the magma will tend to crystallize. Thus, reaction of magma with limestone would tend to cause crystallization of the magma, as discussed by Wyllie (in press). However, because of low permeability of rocks and slow rate of diffusion of H_2O in the magma (Burnham, 1967), reaction between wall rock and magma probably would be restricted to the immediate zone of contact.

ACKNOWLEDGMENTS

I thank Dr. C. Wayne Burnham for his guidance in the Ph.D. thesis project from which this paper is in part derived. The experimental work was supported by NSF grants GA-1110 and GA-3952 to Dr. Burnham. I thank also Dr. P. J. Wyllie and Dr. J. K. Robertson for their helpful suggestions in preparation and review of this manuscript.

REFERENCES

- Barker, D. S., 1965, Alkalic rocks at Litchfield, Maine: *Jour. Petrology*, v. 6, p. 1-27.
- Bell, P. M., and Roseboom, E. H., 1969, Melting relationships of jadeite and albite to 45 kilobars with comments on melting diagrams of binary systems at high pressures: *Mineralog. Soc. America Spec. Paper* 2, p. 151-161.
- Burnham, C. W., 1962, Large volume apparatus for high-temperature high-pressure experimentation: *Am. Ceramic Soc. Mtg.*, Seattle, 1962, Program.
- 1967, Hydrothermal fluids at the magmatic stage, in Barnes, H. L., ed., *Geochemistry of hydrothermal ore deposits*: New York, Holt, Rinehart and Winston, Inc., p. 34-76.
- Burnham, C. W., Holloway, J. R., and Davis, N. F., 1969a, The specific volume of water in the range 1000 to 8900 bars, 20° to 900°C: *Am. Jour. Sci.*, v. 267-A, Schairer v., p. 70-95.
- 1969b, Thermodynamic properties of water to 1000°C and 10,000 bars: *Geol. Soc. America Spec. Paper* 132, 96 p.
- Greenwood, H. J., 1961, The system $\text{NaAlSi}_3\text{O}_8\text{-H}_2\text{O-Argon}$: Total pressure and water pressure in metamorphism: *Jour. Geophys. Research*, v. 66, p. 3923-3946.
- Hamilton, D. L., and MacKenzie, W. S., 1965, Phase equilibrium studies in the system $\text{NaAlSi}_3\text{O}_8\text{-(nepheline)-KAlSi}_3\text{O}_8\text{-(kalsilite)-SiO}_2\text{-H}_2\text{O}$: *Mineralog. Mag.*, v. 34, p. 214-231.
- Hill, R. E. T., and Boettcher, A. L., 1970, Water in the earth's mantle: Melting curves of basalt-water and basalt-water-carbon dioxide: *Science*, v. 167, p. 980-982.
- Holloway, J. R., ms, 1970, Phase relations and compositions in the basalt- $\text{CO}_2\text{-H}_2\text{O}$ system at high temperatures and pressures: Ph.D. thesis, Pennsylvania State University, University Park, Pa.
- Holloway, J. R., Burnham, C. W., and Millhollen, G. L., 1968, Generation of $\text{H}_2\text{O-CO}_2$ mixtures for use in hydrothermal experimentation: *Jour. Geophys. Research*, v. 73, p. 6598-6600.
- Keith, M. L., 1939, Petrology of the alkaline intrusive at Blue Mountain: *Geol. Soc. America Bull.*, v. 50, p. 1795-1826.
- Millhollen, G. L., ms, 1970, Melting and phase relations in nepheline syenites with H_2O and $\text{H}_2\text{O} + \text{CO}_2$: Ph.D. thesis, Pennsylvania State University, University Park, Pa.
- Morse, S. A., 1969, Syenites: *Carnegie Inst. Washington Year Book* 67, p. 112-120.
- Nockolds, S. R., 1954, Average chemical compositions of some igneous rocks: *Geol. Soc. America Bull.*, v. 65, p. 1007-1032.
- Payne, J. G., 1968, Geology and geochemistry of the Blue Mountain nepheline syenite: *Canadian Jour. Earth Sci.*, v. 5, p. 259-273.
- Peters, Tj., Luth, W. C., and Tuttle, O. F., 1966, The melting of analcite solid solutions in the system $\text{NaAlSi}_3\text{O}_8\text{-NaAlSi}_2\text{O}_6\text{-H}_2\text{O}$: *Am. Mineralogist*, v. 51, p. 736-753.
- Schairer, J. F., 1950, The alkali feldspar join in the system $\text{NaAlSi}_3\text{O}_8\text{-KAlSi}_3\text{O}_8\text{-SiO}_2$: *Jour. Geology*, v. 58, p. 512-517.
- Tuttle, O. F., 1949, Two pressure vessels for silicate-water studies: *Geol. Soc. America Bull.*, v. 60, p. 1727-1729.
- Watkinson, D. H., and Wyllie, P. J., 1969, Phase equilibrium studies bearing on the limestone assimilation hypothesis: *Geol. Soc. America Bull.*, v. 80, p. 1565-1576.
- Wyllie, P. J., in press, Limestone assimilation, in Sorenson, H., ed., *The alkaline rocks*: New York, Intersci. Publishers.
- Wyllie, P. J., and Tuttle, O. F., 1959, Effect of carbon dioxide on the melting of granite and feldspars: *Am. Jour. Sci.*, v. 257, p. 648-655.
- 1960, Experimental investigation of silicate systems containing two volatile components. Part I. Geometrical considerations: *Am. Jour. Sci.*, v. 258, p. 498-517.
- Yoder, H. S., and Tilley, C. E., 1962, Origin of basalt magmas: An experimental study of natural and synthetic rock systems: *Jour. Petrology*, v. 3, p. 342-532.